Asian Journal of Chemistry; Vol. 36, No. 2 (2024), 371-376

ASIAN JOURNAL OF CHEMISTRY

https://doi.org/10.14233/ajchem.2024.30951

Impact of Al^{3+} Ions Incorporation on the Enhancement of Optical and Electrical Properties of Cadmium Oxalate Crystals

A.S. GANAVI[1], N. JAGANNATHA[1,*], K.P. NAGARAJA[2], DELMA D'SOUZA[2] and P.S. ROHITH[2]

[1]Department of Physics, University College Mangalore (A Constituent College of Mangalore University), Mangalore-575001, India
[2]Department of Physics, Field Marshal K.M. Cariappa College, Madikeri-571201, India

*Corresponding author: E-mail: jagannathnettar64@gmail.com

Received: 24 November 2023; *Accepted*: 29 December 2023; *Published online*: 31 January 2024; AJC-21524

Aluminium (impurity ion) incorporated cadmium oxalate (ACO) crystals were grown in a silica hydrogel media by diffusion technique. ACO crystals emerged with the dimension 6 mm × 2 mm × 1.5 mm at the optimizing parameters of gel pH 4.2, gel density 1.01 g cm^{-3}, sodium metasilicate (SMS):oxalic acid of 5:4 and supernatant mixture at an equal ratio (1:1). Further, the extracted crystals were analyzed by employing energy dispersive X-ray analysis (EDAX), Fourier transform infrared (FTIR) spectroscopy and thermogravimetric (TG) studies. EDAX measurements confirmed the presence of cations at the ratio Cd^{2+}:Al^{3+} = 65.67:1, whereas FTIR spectra identified O-H, C-C, C-O, C=O and M-O bonds in the crystal armature. TG analysis showed two decomposition phases of foregrounded crystals with thermal stability up to 1076.79 ºC in the metal oxide state with minimum change in entropy (ΔS = -266.95 J mol^{-1} K^{-1}). The ACO crystal crystallized in a triclinic system. The optical and electrical behaviours of ACO crystals were compared with pure cadmium oxalate crystals. ACO crystals showed complete transparency to visible light and maximum absorption in the UV region like pure/parent crystals but the energy gap E_g was reduced to 5.90 eV. The leakage resistance R_L of ACO crystals was also reduced to 6.583 GΩ and the electrical conductivity coefficient σ_k was enhanced to 0.152 S m^{-1} ºC^{-1} from parent cadmium oxalate crystals.

Keywords: Energy gap, Leakage resistance, Oxalate crystals, Silica hydrogel.

INTRODUCTION

Current trends in the field of science and technology in general and crystallography in particular is, growing optimum size doped/mixed crystals of divalent and trivalent cations for optical and electrical applications. Crystal growth is a unique field of research in science, where highest ordered substances are developed. Of the various crystal growth methods, crystals grown from gels stand unique because of their special properties like water insolubility, purity, mechanical strength and thermal stabilities [1-4]. The literature review has reported the growth kinetics and properties of many pure, doped and mixed crystals. In particular, oxalate crystals showed the optical and electrical applications [5-9]. Hence, by noting the adaptability of oxalate anion with various metal cations the present work focuses on the growth of trivalent ion, Al^{3+} incorporated cadmium oxalate crystals and the study on modification caused by Al^{3+} impurity in the optical and electrical properties of pure/parent cadmium oxalate crystals.

EXPERIMENTAL

Crystal growth: Aluminium (impurity ion) incorporated cadmium oxalate (ACO) crystals were grown at laboratory conditions by employing the chemical reaction method of gel technique [10]. Crystal growth in gels was accomplished by optimizing the gel media. The optimal growth condition was achieved by amalgamating sodium metasilicate (SMS) solution (specific gravity = 1.0375 g cm^{-3}) and oxalic acid (concentration = 0.5 M) for the ratio 5:4 at 26 ºC in turn to obtain oxalic acid impregnated silica (OIS) hydrogel. Al^{3+} and Cd^{2+} cation mixture (1:1) in their nitrate form were diffused through polymerized OIS gel (gel set duration = 5 days) nucleated with $C_2O_4^{2-}$ ions that existed in the gel and produced as ACO crystals. Table-1 records the growth parameters of ACO crystals. The growth aspects of ACO crystals (Fig. 1) revealed that trivalent Al^{3+} cationic mixing to Cd^{2+} ions vacancies increased the surface fineness and transparency to light, which would induce improved optical activity.

TABLE-1
OPTIMIZED GROWTH PARAMETERS: ACO CRYSTALS

Growth parameters	Particulars of ACO crystals
Specific gravity of SMS solution (g cm^{-3})	1.0375
Concentration of oxalic acid (M)	0.5
Ratio of SMS: Oxalic acid	5:4
pH of the gel	4.2
Gel density (g cm^{-3})	1.01
Concentration of supernatant solutions (M)	0. 5
Ratio of cationic reactants	1:1
Duration of crystal growth (days)	15
Size {l × b × h (mm^3)}	6 × 2 × 1.5
Colour	Colourless
Physical appearance	Transparent and hard

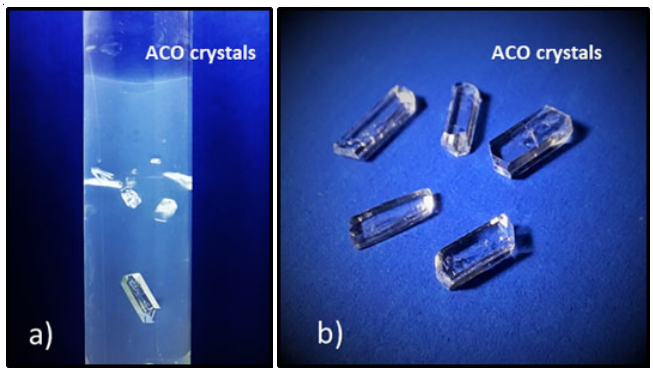

Fig. 1. (a) Growth of ACO crystals *in silica* hydrogel and (b) Extracted crystals

Characterization: The elemental composition in the ACO crystal was identified by EDAX with the help of CARL ZEISS FESEM attached EDS system. FTIR spectrum ranging from 4000-400 cm^{-1} was obtained from the Thermo Nicolet iS50 FTIR spectrometer. TG studies were carried out using TGA-DTA (Hitachi STA 7300). Bruker D8 Advance A25 diffractometer was used to obtain Bragg's diffraction pattern to visualize the pattern powderX software was used and the diffraction peaks were indexed using N-treor-09 program and CHEKCELL software to obtain lattice parameters. Optical and electrical properties of ACO crystals were determined using UV-VIS-NIR θ/2θ spectrophotometer (HO-SPA-1990P) followed by two probe method and electrical conductivity by Roy instruments (IR 503).

RESULTS AND DISCUSSION

EDAX-FESEM studies: The X-ray characteristic peaks and area under the spectral lines of the EDAX spectrum have confirmed the presence of oxygen, carbon, cadmium and aluminium in the ACO crystal (Fig. 2a). The FESEM image at 100 µm resolution (Fig. 2b) showed different ordered layers with valley regions [11]. The weight and atomic percentages of elements present in the foregrounded crystals are listed in Table-2. The EDAX measurements confirmed the cationic distribution of Cd^{2+}:Al^{3+} in the ratio 65.67:1. The addition of Al^{3+} (impurity) into Cd^{2+} vacancies preserved the original shape of pure cadmium oxalate crystals with different dimensions [6].

TABLE-2
CHEMICAL CONSTITUENTS OF ACO CRYSTALS

Elements	Weight (%)	Atomic (%)
Cd	40.15	8.06
Al	0.15	0.12
O	43.41	61.21
C	16.29	30.61
Total	100	100

FTIR studies: Fig. 3 illustrates the FTIR spectrum of ACO crystals and the band assignments are listed in Table-3. The broad band ranging from 3500.65 to 3195.49 cm^{-1} exhibited the symmetric and asymmetric stretching of the O-H group, which confirmed the presence of water molecules. The strong asymmetrical band at 1570.50 cm^{-1} was due to C=O stretching. The sharp absorption peak at 1312.70 cm^{-1} indicated the C-C vibrations and C-O stretching. The absorption bands at 782.69 and 707.26 cm^{-1} were due to O-H bending. The absorption peaks at 560.22 and 444.23 cm^{-1} correspond to M-O stretching in ACO crystals [12,13]. FTIR spectral analysis of ACO crystals reveals the shift in the absorption band but retained the pure

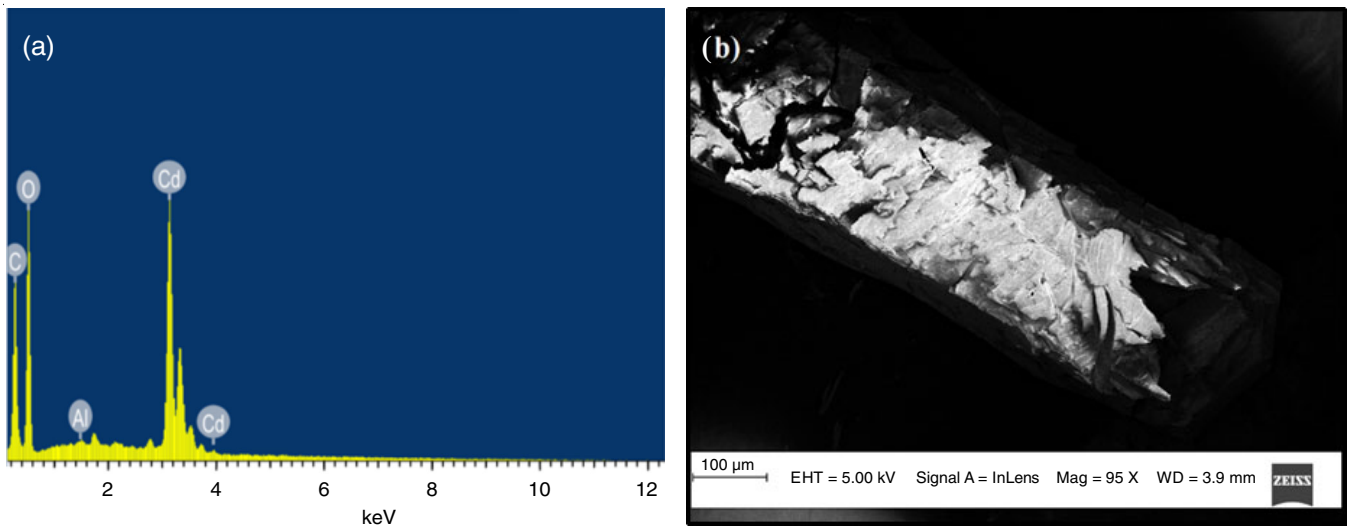

Fig. 2. (a) EDAX spectrum and (b) FESEM image: ACO crystals

TABLE-3
BAND ASSIGNMENTS OF ACO CRYSTALS

Band assignments	Wavenumbers (cm^{-1})
Symmetric and asymmetric stretching of OH group and water of crystallization	3500.65, 3420.42, 3195.49
C=O stretching, O-H bending	1570.50
C-C vibrations, C-O stretching	1312.70
O-H out of plane bending, M-O bonding	782.69, 707.26
M-O stretching	560.22, 444.23

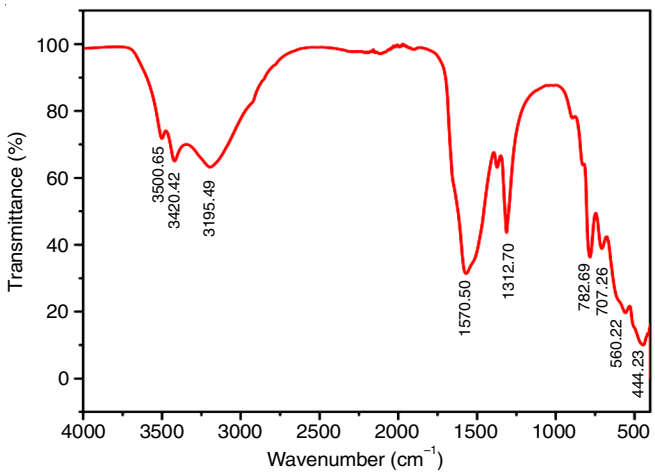

Fig. 3. FTIR spectrum of ACO crystals

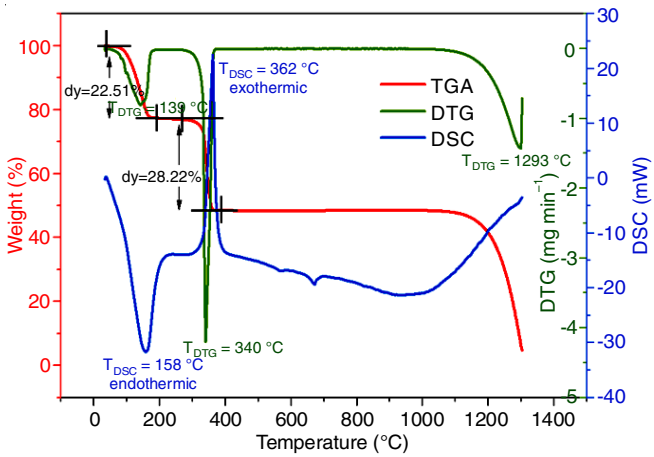

Fig. 4. TG studies of ACO crystal

crystals armature [6]. The shift in the absorption band confirms Al^{3+} ion occupation into Cd^{2+} vacancies.

Thermogravimetric (TG) studies: The decomposition behaviour and thermal stabilities of ACO crystals were studied by thermogravimetric analysis (TGA), derivative thermogravimetry (DTG) and differential scanning calorimetry (DSC). These TG studies determined the decomposition temperatures (T_D), rate of weight loss (%) and chemical processes involved during the decomposition of ACO crystals. Fig. 4 shows two structural transformations of novel crystals. In the first phase of decomposition, the crystal lost three water molecules with a weight loss of 22.51% (calculated weight loss 21.34%) for the temperature range (T_D = 33.78-192.80 ºC), which leads to T_{DTG} peak at 139 ºC and endothermic T_{DSC} peak at 158 ºC, respectively. The second phase of degradation occurs at T_D = 268.79-384.28 ºC with a T_{DTG} peak at 340 ºC and an exothermic T_{DSC} peak at 362 ºC with a weight loss of 28.22% (calculated loss: 28.44%) due to the degradation of CO and CO_2 molecules simultaneously [14,15]. The TGA curve clearly indicated the enhancement in the thermal stability of ACO crystals up to 1076.79 ºC in the Cd:Al-O state (T_{DTG} = 1293 ºC) [6]. Table-4 provides the TG profile of ACO crystals. The TG studies followed by the evaluation from EDAX and FTIR measurements, the ACO crystal possesses a molecular formula $Cd_{0.985}Al_{0.015}(C_2O_4)\cdot 3H_2O$ with molecular weight of 253.1945.

The TG studies were extended to the degradation phases of ACO crystals. The activation energy, frequency factor, change in entropy, change in enthalpy and change in Gibb's free energy during two stages of decomposition were measured.

The kinetic and thermodynamic parameters of degradation phases were calculated using Coats and Redfern method [16,17]. Eqns. 1 and 2 are for orders of reaction n = 1.

$$\log\left(\frac{-\log(1-\alpha)}{T^2}\right) = \log\left[\left(\frac{AR}{\beta E_a}\right)\left(1-\frac{2RT}{E_a}\right)\right] - \frac{E_a}{2.303RT} \quad (1)$$

where α = fraction of sample (crystals) decomposed.

$$\alpha = \frac{W_o - W_t}{W_o - W_f} \quad (2)$$

where W_t = weight of the sample at any given temperature, W_o = weight of the sample at the initial temperature, W_f = weight of sample at the end of decomposition, β = heating rate, T = absolute temperature, A = frequency factor, E_a = activation energy and R = universal gas constant.

The plots of log [-log(1-α)/T^2] *vs.* 1000/T of phase 1 and phase 2 are shown in Fig. 5. The slope of the plot in turn yielded the activation energy (E_a) and the frequency factor (A) was calculated by using the intercept value.

In terms of E_a and A values, the change in entropy (ΔS), change in enthalpy (ΔH) and the change in Gibbs free energy (ΔG) were calculated using eqns. 3-5 and reported in Table-5.

TABLE-4
DEGRADATION BEHAVIOUR: ACO CRYSTALS

Phase	Decomposition temperature (T_D, °C)	T_{DTG} (°C)	T_{DSC} (°C)	Weight loss (%)		Decomposition phase
				Observed	Calculated	
I	33.78-192.80	139	158	22.51	21.34	$(Cd_{0.985}Al_{0.015})\ C_2O_4\cdot 3H_2O \rightarrow (Cd_{0.985}Al_{0.015})\ C_2O_4 + 3H_2O$
II	268.79-384.28	340	362	28.22	28.44	$(Cd_{0.985}Al_{0.015})\ C_2O_4 \rightarrow (Cd_{0.985}Al_{0.015})\ O + CO + CO_2$

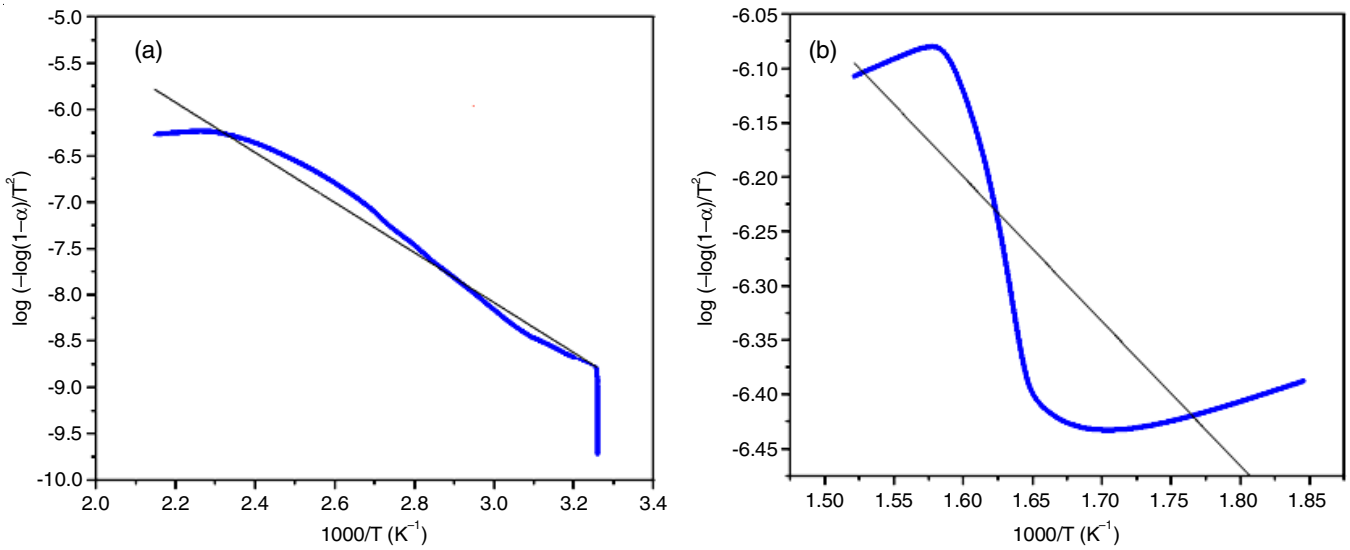

Fig. 5. Coats and Redfern method for degradation phase: (a) Phase 1 and (b) Phase 2

TABLE-5
KINETIC AND THERMODYNAMIC PARAMETERS

Phase	Activation energy (E_a, kJ mol^{-1})	Frequency factor (A, min^{-1})	Entropy change (ΔS, J mol^{-1} K^{-1})	Enthalpy change (ΔH, kJ mol^{-1})	Change in Gibbs free energy (ΔG, kJ mol^{-1})
I	51.74	1.51×10^5	-182.48	48.32	123.52
II	25.49	8.70	-266.95	20.39	184.07

$$\Delta S = R \ln\left(\frac{Ah}{k_B T}\right) \quad (3)$$

$$\Delta H = E_a - RT \quad (4)$$

$$\Delta G = \Delta H - T\Delta S \quad (5)$$

where R = universal gas constant, h = Plank's constant and k_B = Boltzmann constant.

Thermodynamic parameters were calculated at the T_{DTG} (peak) temperature of each phase.

PXRD studies: The resulting PXRD pattern for the specific 2θ values showed a high crystalline nature (Fig. 6) of crystals [18]. ACO crystal crystallized in a triclinic crystal system and retained the structure of the parent cadmium oxalate crystal [6]. Unit cell parameters of ACO crystal are recorded in Table-6.

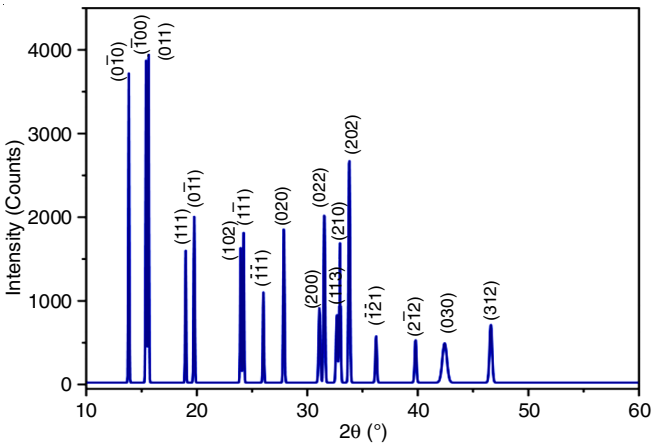

Fig. 6. Bragg's diffraction pattern of ACO crystals

TABLE-6
UNIT CELL PARAMETERS OF ACO CRYSTAL

Cell parameters	Particulars	Cell parameters	Particulars
a (Å)	5.9922	β (°)	74.33
b (Å)	6.6550	γ (°)	80.99
c (Å)	8.4760	Space group	P1
α (°)	74.63	Crystal system	Triclinic

Characterization results of ACO crystals confirmed Al^{3+} impurity ion occupation into Cd^{2+} pure cation vacancies with unaltered triclinic geometry. Al^{3+} cation mixing with Cd^{2+} ions increased the thermal stability with a change in entropy (minimum) during the degradation process; which would promote Al^{3+} incorporation into the parental sites of cadmium oxalate crystals to design a better optical device. Hence, the distinctness in optical and electrical properties of ACO crystals are compared with pure cadmium oxalate crystals [6].

Optical properties: Optical studies of ACO crystals were carried out by subjecting the crystal (solution form) to UV-visible light for absorption (wavelength range 190-900 nm). ACO crystals dissolved in 1.5 N H_2SO_4 heated to 80 ºC for 20 min. After calibration, the crystal exhibited maximum absorption in the UV region with λ_m (wavelength corresponds to maximum absorption A_{max} = 1.538) equals 198 nm (Fig. 7). The crystal solution showed complete transparency in the visible region. The Tauc plot (graph of $(\alpha h\nu)^2$ *vs*. hν) measured the optical band energy E_g = 5.90 eV for ACO crystals. The reduced E_g values for ACO crystal (5.90 eV) from that of pure crystal (6.11 eV) [6] indicate that both the crystals are distinct and insulators. Even though these are insulators, a lower value E_g for ACO crystal would enhance its electrical conductivity.

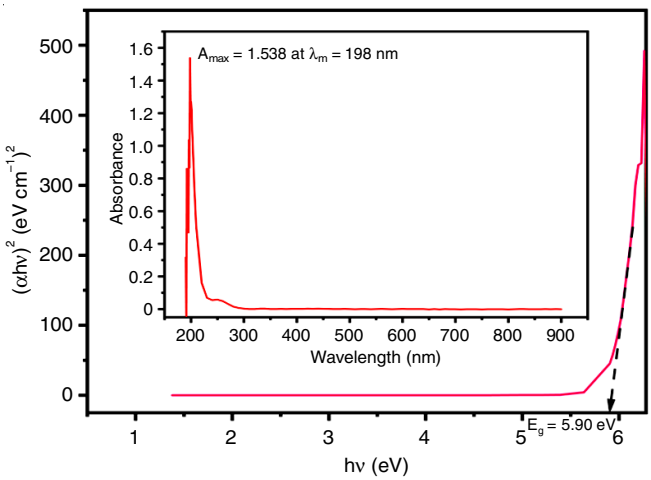

Fig. 7. UV-visible spectrum of ACO crystals

The UV-visible spectral studies of ACO crystals measured higher refractive index n = 1.817 and reflectance R = 0.084 than pure cadmium oxalate crystals (n = 1.782 and R = 0.079); which were measured using eqns. 6 and 7 [19,20]:

$$E_g e^n = 36.3 \quad (6)$$

$$R = \left(\frac{n-1}{n+1}\right)^2 \quad (7)$$

where E_g = band gap energy, n = refractive index and R = reflectance.

Electrical properties: The Volt-ampere (V-I) characteristic of ACO crystal was measured by two probe method. The crystal exhibited linear variation of current with applied DC voltage (Fig. 8a) and the reciprocal of the slope of straight-line measured leakage resistance R_L = 6.583 GΩ. The electrical conductivity also varied linearly with temperature (Fig. 8b) whose electrical conductivity coefficient σ_k = 0.152 S m^{-1} ºC^{-1}. Hence, the crystal behaves as a perfect insulator [5,21].

The optical and electrical properties of pure cadmium oxalate crystals [6,21] are compared with the data obtained for ACO crystals as listed below in Table-7. The characterization results, optical and electrical studies of ACO crystals reveal that the impurity addition (Al^{3+}) to pure crystal reduced band gap energy by an amount of 0.21 eV (6.11 to 5.90 eV). Also, a decrease in leakage resistance R_L = 6.583 GΩ (pure cadmium oxalate R_L = 7.707 GΩ) and an increment in electrical conductivity coefficient σ_k = 0.152 S m^{-1} ºC^{-1} (pure cadmium oxalate σ_k = 0.092 S m^{-1} ºC^{-1}) were observed.

Conclusion

Aluminium incorporated cadmium oxalate crystals (ACO) were grown *in silica* hydrogel media by diffusion method. During diffusion Al^{3+} ions incorporated into the Cd^{2+} ions lattice and formed good quality crystals. Extracted ACO crystals subjected to EDAX measurements confirmed the cationic distribution as Cd^{2+}:Al^{3+} = 65.67:1. FTIR spectral analysis identified the C=O, C-C, C-O, O-H and M-O bonds in crystal armature. Thermal studies confirmed the stability of the ACO crystal up to 1076.79 ºC in the oxide state. The crystal with molecular formula $Cd_{0.985}Al_{0.015}(C_2O_4)\cdot 3H_2O$ and molecular weight of 253.1945 remained in the triclinic system (unaltered from pure crystal). Al^{3+} impurity ion incorporation caused the optical band gap energy to decrease to 5.90 eV from 6.11 eV, increment in refractive index (1.782 to 1.817) and reflectance (0.079 to 0.084). Further, the electrical properties also varied *i.e.* reduced leakage resistance (7.707-6.583 GΩ) and enhancement in electrical

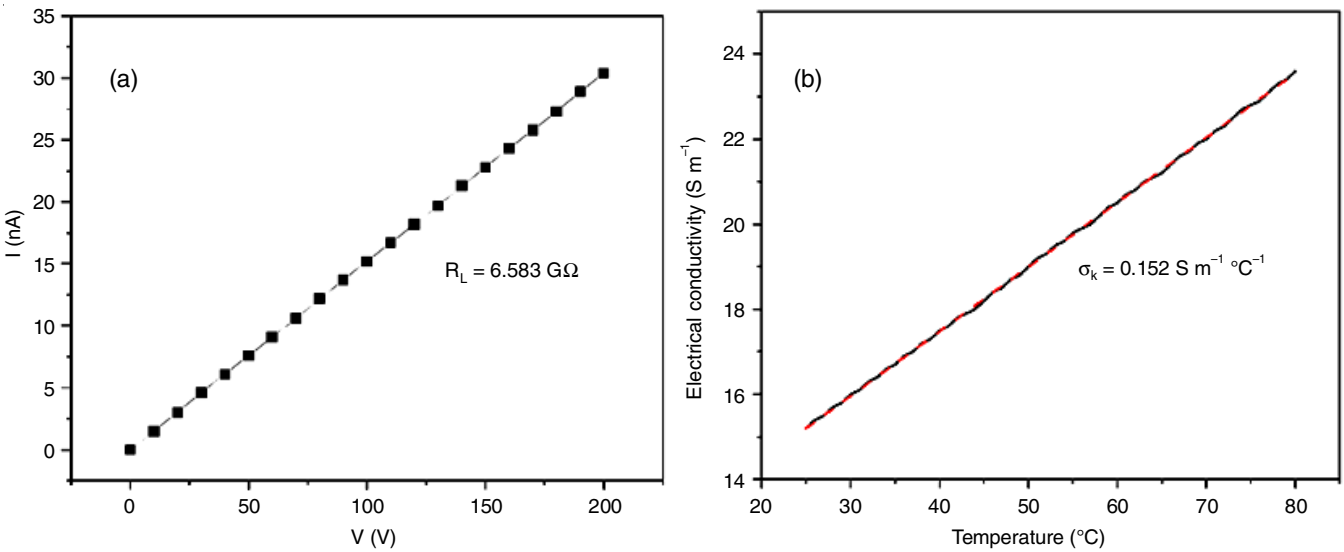

Fig. 8. (a) V-I characteristic and (b) electrical conductivity: ACO crystals

TABLE-7
OPTICAL AND ELECTRICAL PARAMETERS OF ACO CRYSTALS

Crystal	Band gap energy (E_g, eV)	Refractive index (n)	Reflectance (R)	Leakage resistance (R_L, GΩ)	Electrical conductivity (σ_k, S m^{-1} °C^{-1})
ACO	5.90	1.817	0.084	6.583	0.152
Pure cadmium oxalate	6.11	1.782	0.079	7.707	0.092

conductivity (0.092 S m^{-1} $°C^{-1}$ to 0.152 S m^{-1} $°C^{-1}$). As a result of variations in physical, chemical, optical-electrical properties, good thermal stability, water insolubility and transparency, the ACO crystals find a spectrum of applications in ceramics, optics and electronics industries.

ACKNOWLEDGEMENTS

The authors are grateful to DST-PURSE laboratory, Mangalore University, Mangalore and STIC laboratory, Cochin University, Cochin, India for providing the laboratory and spectral facilities.

CONFLICT OF INTEREST

The authors declare that there is no conflict of interests regarding the publication of this article.

REFERENCES

1. P.V. Dalal, K.B. Saraf and S. Shah, *Cryst. Res. Technol.*, **44**, 36 (2009); https://doi.org/10.1002/crat.200800221
2. P.S. Rohith, N. Jagannatha and K.V. Pradeep Kumar, *Mater. Today Proc.*, **8**, 85 (2019); https://doi.org/10.1016/j.matpr.2019.02.084
3. B.B. Parekh, P.M. Vyas, S.R. Vasant and M.J. Joshi, *Bull. Mater. Sci.*, **31**, 143 (2008); https://doi.org/10.1007/s12034-008-0025-1
4. A.M. Ezhil Raj, D.D. Jayanthi and V.B. Jothy, *Solid State Sci.*, **10**, 557 (2008); https://doi.org/10.1016/j.solidstatesciences.2007.10.019
5. D. D'Souza and K.P. Nagaraja, *Cryst. Res. Technol.*, **57**, 2100138 (2022); https://doi.org/10.1002/crat.202100138
6. N. Ponnappa, J. Nettar, H. Mylnahalli, D. D'Souza and L. Neratur, *Cryst. Res. Technol.*, **53**, 1700261 (2018); https://doi.org/10.1002/crat.201700261
7. N. Jagannatha and P. Mohan Rao, *Bull. Mater. Sci.*, **16**, 365 (1993); https://doi.org/10.1007/BF02759549
8. N.V. Prasad, G. Prasad, T. Bhimasankaram, S.V. Suryanarayana and G.S. Kumar, *Bull. Mater. Sci.*, **19**, 639 (1996); https://doi.org/10.1007/BF02745154
9. P.S. Rohith, N. Jagannatha and K.V. Pradeep Kumar, *Bull. Mater. Sci.*, **44**, 185 (2021); https://doi.org/10.1007/s12034-021-02486-3
10. K.P. Nagaraja, D. D'Souza, K.J. Pampa and N.K. Lokanath, *Mater. Res. Express*, **6**, 035506 (2018); https://doi.org/10.1088/2053-1591/aaf309
11. P.S. Rohith, N. Jagannatha and K.V. Pradeep Kumar, *J. Mater. Environ. Sci.*, **11**, 788 (2020).
12. A.M. Ezhil Raj, D.D. Jayanthi, V.B. Jothy, M. Jayachandran and C. Sanjeeviraja, *Inorg. Chim. Acta*, **362**, 1535 (2009); https://doi.org/10.1016/j.ica.2008.07.025
13. E.D. Bacce, A.M. Pires, M.R. Davalos and M. Jafelicci Jr., *Int. J. Inorg. Mater.*, **3**, 443 (2001); https://doi.org/10.1016/S1466-6049(01)00047-2
14. A.S. Ganavi, S.M. Dharmaprakash, N. Jagannatha, K.P. Nagaraja and Delma D'Souza, *Int. J. Innov. Res. Phys.*, **2**, 1 (2021).
15. F. Daisy Selasteen, S. Alfred Cecil Raj, A. Alagappa Moses, F. Emalda Prince, R. Esther Getsy and R. Elakkiya, *J. Cryst. Process Technol.*, **6**, 65499 (2016); https://doi.org/10.4236/jcpt.2016.62002
16. P.V. Dalal, K.B. Saraf, N.G. Shimpi and N.R. Shah, *J. Cryst. Pro. Technol.*, **2**, 156 (2012); https://doi.org/10.4236/jcpt.2012.24023
17. A.B. Kulkarni, S.N. Mathad and R.P. Bakale, *Ann. Chem.*, **30**, 60 (2019); https://doi.org/10.2478/auoc-2019-0011
18. K.P. Nagaraja, K.J. Pampa, S.R. Kumara Swamy and N.K. Lokanath, *J. Appl. Chem.*, **7**, 863 (2018).
19. F.D. Selasteen, S.A. Cecil Raj, A. Anitha, J. John, T. Lavanya and J.F. Rachel, *ISOR J. Appl. Phys.*, **10**, 26 (2018).
20. P. Vasudevan, S. Sankar and D. Jayaraman, *Bull. Korean Chem. Soc.*, **34**, 128 (2013); https://doi.org/10.5012/bkcs.2013.34.1.128
21. K.P. Nagaraja, Ph.D. Thesis, Department of Studies in Physics, University of Mysore, Mysuru, India (2019).